



# **Submarine Pressure Hull Collapse Considering Corrosion and Penetrations**

*Liam Gannon*

**Defence R&D Canada – Atlantic**

Technical Memorandum  
DRDC Atlantic TM 2010-246  
November 2010

This page intentionally left blank.

# **Submarine Pressure Hull Collapse Considering Corrosion and Penetrations**

Liam Gannon

**Defence R&D Canada – Atlantic**

Technical Memorandum

DRDC Atlantic TM 2010-246

November 2010

Principal Author

*Original signed by Liam Gannon*

---

Liam Gannon

Defence Scientist

Approved by

*Original signed by Neil Pegg*

---

Neil Pegg

Head/Warship Performance

Approved for release by

*Original signed by Ron Kuwahara for*

---

Calvin Hyatt

DRP Chair

© Her Majesty the Queen in Right of Canada, as represented by the Minister of National Defence, 2010

© Sa Majesté la Reine (en droit du Canada), telle que représentée par le ministre de la Défense nationale, 2010

## Abstract

---

The influence of corrosion around a casting in a submarine pressure hull is investigated using nonlinear finite element modelling techniques. The area encompassed by the corrosion patch and the percentage thinning of the pressure hull due to corrosion are varied. For each variation in corrosion patch dimensions, collapse pressures are calculated with and without a ballast pump valve body casting located at the center of the corrosion patch. The extent to which the presence of the casting within a corrosion patch influences collapse pressure is examined and different methods of modelling the casting within the pressure hull are evaluated. The loss of strength caused by corrosion is largely counteracted by the presence of a casting in the corroded region. The casting stiffens the response of the shell plating in that area, causing an increase in collapse pressure. The benefit provided by the casting increased as the percentage thinning of the shell plating increased, increasing the failure load of the corroded hull by as much as 19% for 20% thinning of the shell plating.

## Résumé

---

On a étudié l'influence de la corrosion présente autour d'une pièce moulée de la coque épaisse d'un sous-marin en utilisant des techniques de modélisation par éléments finis non linéaires. Les paramètres variables sont la surface de la zone de corrosion et le pourcentage d'amincissement de la coque épaisse causé par la corrosion. Des valeurs de la pression d'écrasement sont calculées pour les diverses dimensions de la zone de corrosion, et ce, dans les cas de présence ou d'absence d'un corps de valve moulé de pompe de ballast situé au centre de la zone de corrosion. On a examiné l'importance des effets de la présence d'une pièce moulée dans une zone de corrosion sur la pression d'écrasement et évalué différentes méthodes de modélisation d'une pièce moulée dans une coque épaisse. La diminution de la résistance causée par la corrosion est en grande partie compensée par la présence d'une pièce moulée dans la zone de corrosion, car la pièce renforce la structure du bordé extérieur dans cette zone, ce qui entraîne un accroissement de la pression d'écrasement. Les avantages associés à la présence de la pièce moulée augmentent avec l'accroissement du pourcentage d'amincissement du bordé extérieur; en pratique, l'augmentation de la charge de rupture de la coque touchée par la corrosion peut atteindre 19 %, pour un amincissement de 20 % du bordé extérieur.

This page intentionally left blank.

## Executive summary

---

### Submarine Pressure Hull Collapse Considering Corrosion and Penetrations

Liam Gannon; DRDC Atlantic TM 2010-246; Defence R&D Canada – Atlantic; November 2010.

**Introduction or background:** Corrosion of submarine pressure hulls has the potential to reduce the collapse pressure and thus the operational limits of a vessel. Although the influence of corrosion on collapse pressure has been studied previously, it is unclear what influence a penetration and casting within a corroded area have on the reduction in collapse pressure due to corrosion.

**Results:** The presence of a casting within a corrosion patch stiffens the response to external pressure in the damaged area, and increases the interframe collapse pressure provided that the out-of-circularity imperfections facilitate collapse at that location. The casting counteracts the effect of thinning to an increasing degree as the percentage thinning of the shell plating increases.

**Significance:** The results of this study provide further insight into how corrosion of a submarine pressure hull influences collapse pressure, which is important in assessing the operational limits of vessels in service. In situations where a casting is present in the corroded region, the presence of the casting largely counteracts the loss of strength caused by the corrosion damage. Corrosion damage to pressure hulls commonly occurs around penetrations and castings. In addition to this important finding, the study also demonstrates methods of accounting for penetrations and castings in pressure hull analysis and their potential influence on pressure hull behaviour under hydrostatic load.

## Sommaire

---

### Submarine Pressure Hull Collapse Considering Corrosion and Penetrations

Liam Gannon; RDDC Atlantique TM 2010-246; R & D pour la défense Canada – Atlantique; novembre 2010.

**Introduction ou contexte :** La corrosion des coques épaisses de sous-marin pourrait entraîner une réduction de la pression d'écrasement et, conséquemment, celle des conditions limites d'exploitation d'un bâtiment. Les effets de la corrosion sur la pression d'écrasement ont déjà fait l'objet d'études antérieures, mais il n'a jamais été possible d'établir clairement quels sont les effets d'une pénétration et d'une pièce moulée présentes dans une zone de corrosion sur la pression d'écrasement causée par la corrosion.

**Résultats :** La présence d'une pièce moulée dans une zone de corrosion renforce la structure de la zone endommagée et sa résistance à la pression extérieure, ce qui entraîne un accroissement de la pression d'écrasement entre les structures, à condition que les imperfections de nature non circulaire facilitent l'écrasement dans cette zone particulière. La résistance à l'écrasement entre les structures qu'offre la pièce moulée augmente avec l'accroissement du pourcentage d'amincissement du bordé extérieur.

**Importance :** Les résultats de la présente étude fournissent une image plus précise des effets de la corrosion subie par une coque épaisse de sous-marin sur la pression d'écrasement, un important élément de l'évaluation des conditions limites d'exploitation des bâtiments en service. Les dommages que cause la corrosion aux coques épaisses se produisent habituellement autour de pénétrations et de pièces moulées. Les travaux de recherche traités dans le présent rapport permettent de démontrer la validité de méthodes qui tiennent compte des pénétrations et des pièces moulées lors de l'analyse des coques épaisses et de leurs effets possibles sur le comportement d'une coque épaisse soumise à une charge hydrostatique.



# Table of contents

---

Abstract .....	i
Résumé .....	i
Executive summary .....	iii
Sommaire .....	iv
Table of contents .....	v
List of figures .....	vi
List of tables .....	vii
1 Introduction.....	1
1.1 Background.....	1
1.2 Geometry .....	1
2 Finite Element Modelling .....	4
2.1 Pressure Hull Model.....	4
2.2 Casting Model .....	6
2.3 Out-of-Circularity.....	7
2.4 Corrosion .....	8
2.5 Boundary Conditions and Loading.....	9
2.6 Validation of the Modelling Method.....	10
2.7 Effect of Out-of-Circularity Phase Alignment .....	11
2.8 Simplifying the casting geometry.....	12
2.9 SubSAS Modelling.....	14
3 Parametric Study.....	17
4 Conclusions.....	19
References .....	20
Annex A ..Load Versus Displacement Curves.....	21
A.1 5% Thinning of Shell Plating .....	21
A.2 10% Thinning of Shell Plating .....	23
A.3 15% Thinning of Shell Plating .....	24
A.4 20% Thinning of Shell Plating .....	26
List of symbols/abbreviations/acronyms/initialisms .....	29
Distribution list .....	31

## List of figures

---

Figure 1, Pressure hull compartment geometry.....	2
Figure 2, Pressure hull out-of-circularity modes .....	2
Figure 3, Valve geometry (t = shell plating thickness).....	3
Figure 4, Finite element mesh of 1/4 pressure hull model .....	4
Figure 5, Solid to shell element interface .....	5
Figure 6, Solid to shell element connection using stiff beams .....	6
Figure 7, Cutaway of meshed valve body casting .....	7
Figure 8, Interframe out-of-circularity (500x).....	8
Figure 9, Overall out-of-circularity (20x).....	8
Figure 10, Casting and corrosion patch.....	9
Figure 11, Displacement boundary conditions .....	10
Figure 12, Radial displacement at the center of the corrosion patch.....	12
Figure 13, Simplified casting geometry .....	13
Figure 14, Radial displacement of casting.....	13
Figure 15, Joining of ANSYS and SubSAS finite element models.....	14
Figure 16, Radial displacement at center of corrosion patch No. 2 with 15% thinning .....	18

## List of tables

---

Table 1, Collapse pressures predicted using different modelling methods .....	11
Table 2, Normalized collapse pressures .....	17
Table 3, Increase in failure load due to presence of casting (%).....	17
Table 4, Decrease in failure load due to corrosion including casting (%).....	17

This page intentionally left blank.

# 1 Introduction

---

## 1.1 Background

The pressure hull of a submarine is primarily designed to resist loads from external hydrostatic pressure applied when the vessel is submerged. Pressure hulls typically consist of cylindrical and conical compartments made from internally stiffened high strength steel plates. The compartments are separated by watertight bulkheads with spherical or torispherical domes capping the ends of the hull.

The operation of submarines in a salt water environment can lead to corrosion if the pressure hull is not sufficiently protected. Corrosion initiation often occurs around penetrations and at locations where acoustic tiles have de-bonded from the shell plating. The degradation of material properties and loss of material due to corrosion has the potential to significantly reduce collapse pressure so that restrictions on the operational limits of a vessel are required. Remedial measures may be taken to repair material damaged by corrosion including:

- Removal and replacement of the damaged material. This can be expensive and time consuming.
- Removal of damaged material by grinding after which the thinned hull plating is built up using several layers of weld metal. This method reclaims lost material, however significant residual stresses and distortions may be introduced by welding.
- Removal of damaged material by grinding with no replacement of lost material.

The influence of thinning due to corrosion on collapse pressure has been investigated both experimentally and numerically [1, 2, 3], however in most cases the corrosion patches were not located near penetrations in the pressure hull. The primary purpose of this study is to determine if the presence of a penetration and casting within a corroded area of a pressure hull alters the behaviour of the structure under external hydrostatic pressure. Finite element techniques for modelling a penetration and casting in a pressure hull with corrosion are developed and a simplified method of representing the casting is evaluated. Pressures at which a serviceability limit state at the casting location is exceeded are compared with and without a penetration for a casting within the corroded area. It is noted that the behaviour of a pressure hull with corrosion in the vicinity of a casting may be different when shock loads are considered and that this is a potential area for future research.

## 1.2 Geometry

A generic cylindrical pressure hull compartment shown in Figure 1 was chosen for the analysis. The compartment consists of 21 bays with 20 tee stiffeners between bulkheads. One and a half bays of shell plating with a single stiffener were added to each side of the compartment to facilitate application of realistic boundary conditions in the finite element model that is described in detail in Section 2.

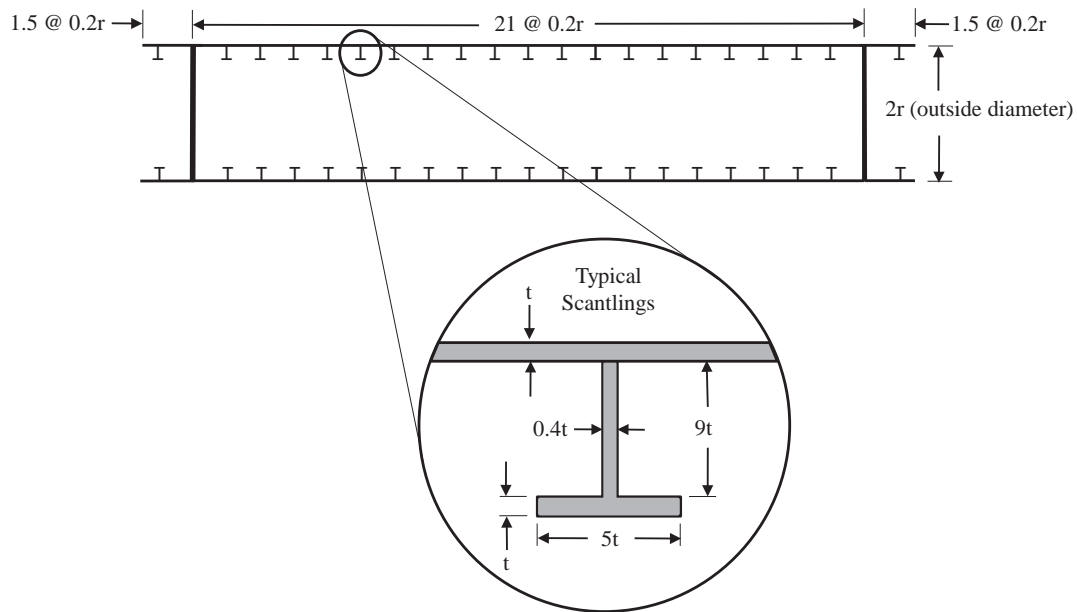


Figure 1, Pressure hull compartment geometry

In order to account for imperfections in the shape of the pressure hull that arise during construction, overall and interframe out-of-circularity (OOC) imperfections were included in the model. The magnitude and distribution of the imperfections were calculated using the British submarine structures design standard, SSP 74 [4]. The design standard was used to determine overall and interframe out-of-circularity mode numbers  $n$ , that result in the minimum collapse pressure for the respective type of failure. These are  $n = 3$  and  $n = 15$  for overall and interframe collapse, respectively. Figure 2 shows the circumferential distribution of the out-of-circularity for both OOC modes. The overall OOC is distributed as a half sine wave between bulkheads and the interframe OOC is distributed in half sine waves between frames that alternate in direction from one bay to the next. The maximum amplitude of the overall out-of-circularity (at the compartment mid-length) was taken as  $0.005r$ , where  $r$ , is the nominal outer radius of the cylinder. The amplitude of interframe OOC was taken as  $0.01t$ , where  $t$  is the thickness of the pressure hull plating.

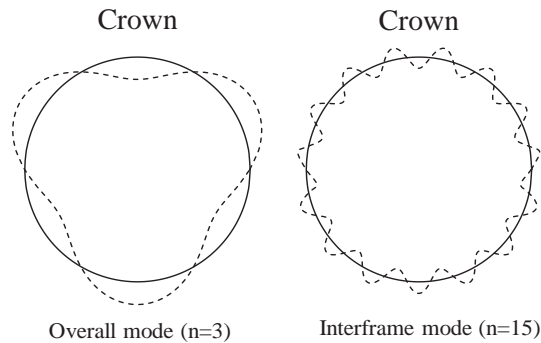


Figure 2, Pressure hull out-of-circularity modes

The casting used in the study was a ballast system valve body. Figure 3 shows the general shape and approximate dimensions of the casting. Both the casting and the center of the corrosion patch are located at the crown of the pressure hull, at the compartment mid-length which is half-way between two frames. The effect of out-of-circularity phase alignment on collapse pressure was evaluated as described in Section 2.3. Based on the results of that evaluation, the phases of the circumferential components of the out-of-circularity modes for all models were aligned at the crown, as shown in Figure 2, so that the troughs of both the overall and interframe modes were aligned with the casting and the center of the corrosion patch. Previous studies have also shown that this alignment of OOC at a corrosion patch has the greatest impact on structural capability [1].

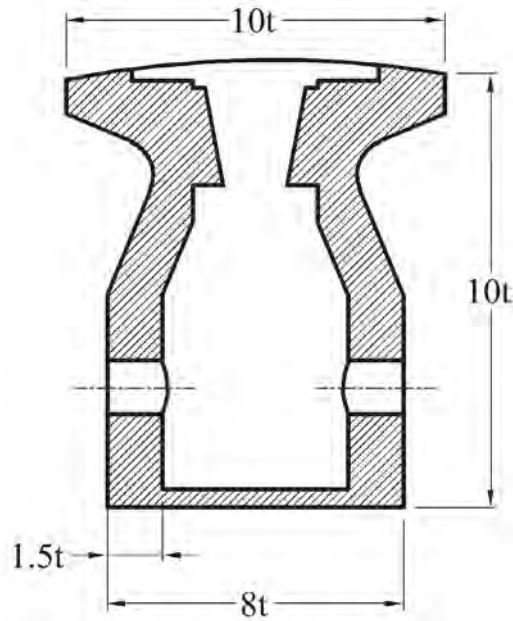


Figure 3, Valve geometry ( $t$  = shell plating thickness)

## 2 Finite Element Modelling

### 2.1 Pressure Hull Model

Finite element modelling was carried out using the ANSYS finite element analysis program. One-quarter of the complete pressure hull was modelled, taking advantage of the longitudinal and transverse symmetry of the model to reduce analysis time. Figure 4 shows the meshed, one-quarter pressure hull model. The three dimensional model used 4-node shell elements with six degrees of freedom at each node ( $u_x$ ,  $u_y$ ,  $u_z$ ,  $rot_x$ ,  $rot_y$ ,  $rot_z$ ) for the majority of the pressure hull shell plating and for the stiffeners. The pressure hull shell plating affected by corrosion and the remaining shell plating up to the nearest stiffener were meshed using 8-node hexahedral solid elements with three degrees of freedom at each node ( $u_x$ ,  $u_y$ ,  $u_z$ ). The volumes meshed with solid elements near the casting were created first by rotating areas about the longitudinal axis of the cylinder. The areas for a single bay of shell plating and a single stiffener were then created and meshed with shell elements. These were copied a number of times to create the rest of the pressure hull.

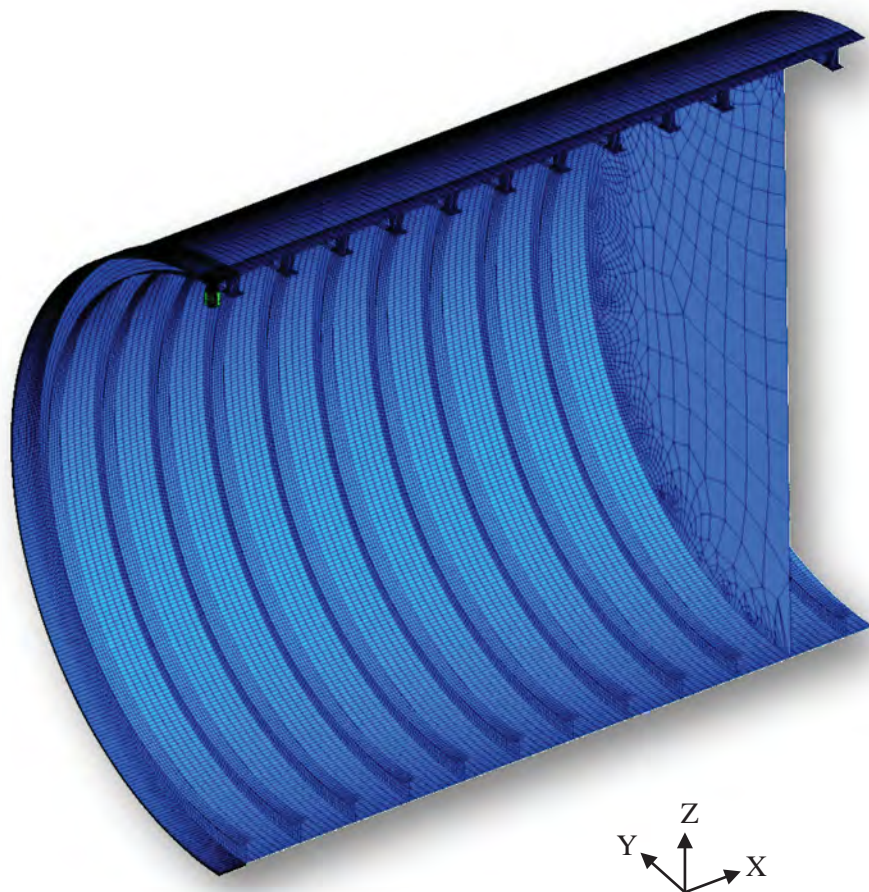
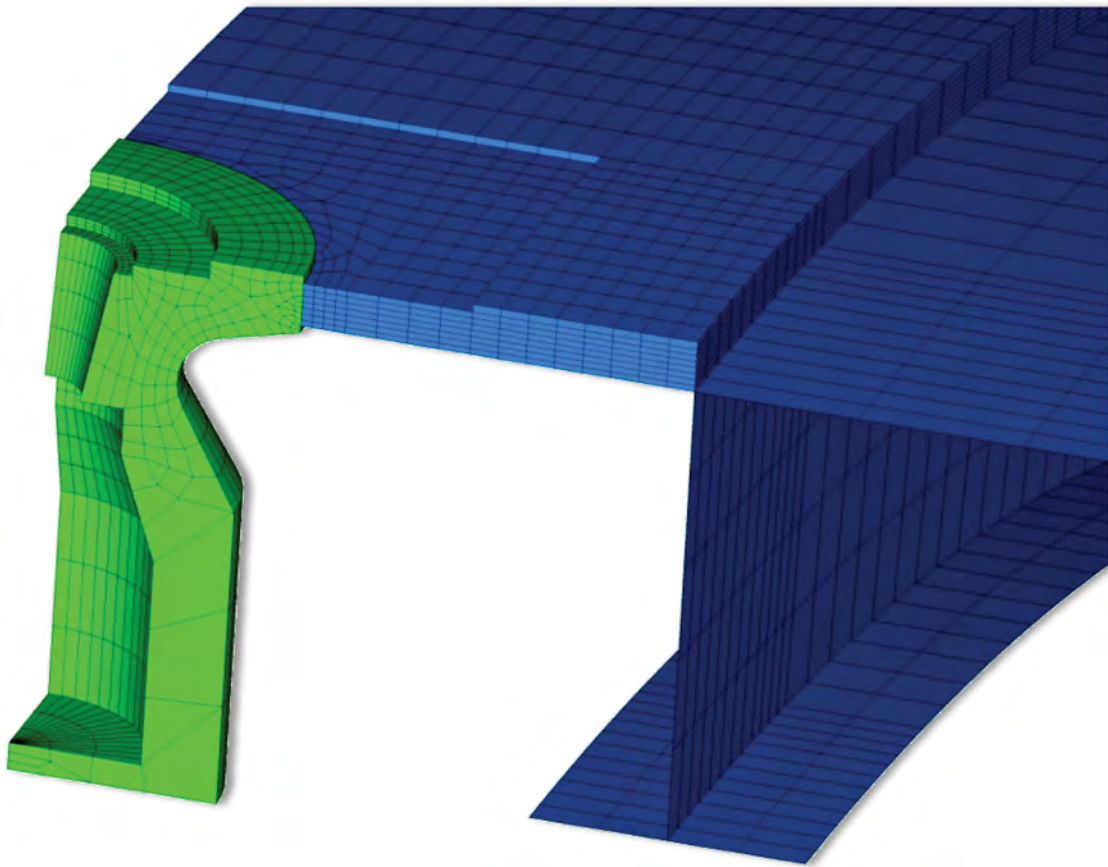


Figure 4, Finite element mesh of 1/4 pressure hull model

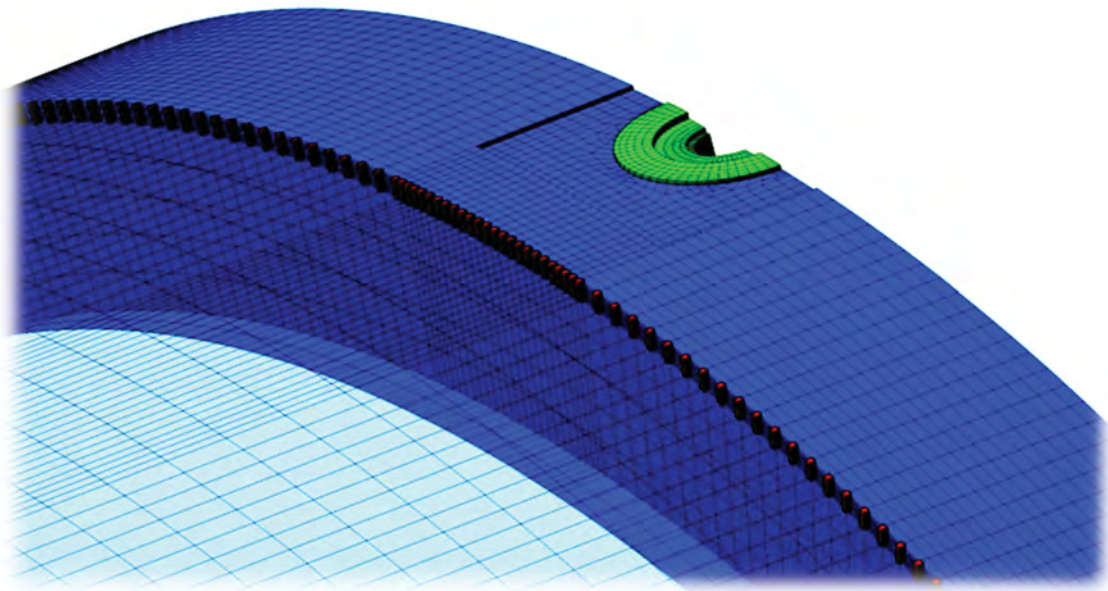


Figure 5 shows a close view of a typical finite element mesh. The shell plating was meshed using 10 elements between stiffeners in the fore-aft direction and 500 elements around the circumference. That portion of the shell plating meshed with solid elements had 8 elements through the thickness in order to accurately model bending of the shell plating and to capture progressive yielding through the thickness of the plating. Ring stiffeners had 6 shell elements through the depth of the web and 4 shell elements across the width of the flange. Solid elements were fully integrated, using the ANSYS enhanced strain formulation to prevent shear locking and the shell elements used reduced integration. Twenty one integration points were used through the thickness of the shell plating and stiffener flange shell elements. All other shell elements had 5 integration points through their thickness. Shell element nodes were offset from the mid-plane of the elements in order to eliminate overlap where the flange and web of the stiffener intersect and also where the web of the stiffeners and the shell plating meet. All pressure hull material, including the casting was assumed to be made from Q1N high strength steel with a yield stress of 550 MPa, elastic modulus of 207 GPa, hardening modulus of 3.2 GPa, and Poisson's ratio of 0.3 [5]. The material was elasto-plastic with a bilinear, isotropic hardening stress-strain relationship.



*Figure 5, Solid to shell element interface*

In order to allow rotations of the pressure hull shell element nodes to be transmitted to the solid elements, stiff linear beam elements were used to tie together regions of the model that were meshed with different element types. This method of joining dissimilarly meshed regions was implemented in such a way that any discontinuity in stresses caused by the transition from one element type to another with different shape functions was minimized. To this end, the shell plating around the casting and corrosion patch was also meshed with solid elements up to the nearest stiffener so that the transition from solids to shells would be farther away from the area of interest, lessening the influence of the transition on the stress field around the casting. In cases where the corrosion patch extended into the bays adjacent to the one with the casting, solid elements were also used to mesh both adjacent bays and the transition to shells was located at the far stiffener in those bays. Figure 6 illustrates the solid to shell element connection, where the elements shown in red are the stiff beam elements and the shell elements making up the shell plating were made translucent for clarity in the figure.



*Figure 6, Solid to shell element connection using stiff beams*

## **2.2 Casting Model**

The casting used for the analysis was a high pressure ballast pump valve casting. The casting was meshed with 8-node hexahedral elements. The geometry was simplified by removing penetrations in the casting for inlets, and by removing the valve. Figure 7 shows the meshed casting. The casting material properties were the same as those used for the pressure hull.

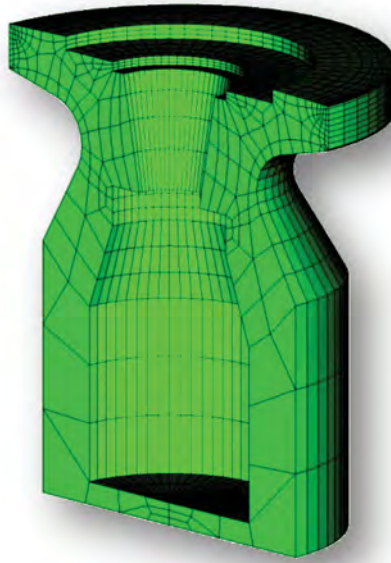


Figure 7, Cutaway of meshed valve body casting

## 2.3 Out-of-Circularity

Out-of-circularity imperfections were added to the model by running a preliminary, linear elastic analysis during which radial displacements were prescribed at each node to produce the desired shape. When the analysis was complete, the nodal coordinates were updated by reading the nodal displacements from the results file and adding them to the initial nodal coordinates (ANSYS UPGEOM command). Radial displacements were calculated for each node using the following trigonometric series to represent the overall and interframe components of the OOC:

$$\Delta_{O,i} = A_O a \sin(\varphi + n\theta) \sin\left(\frac{\pi}{2} + \frac{\pi x}{2L}\right) \quad (1)$$

$$\Delta_{I,i} = A_I \sin(\varphi + n\theta) \sin\left(\frac{\pi}{2} + x(\text{mod} L_B)\pi\right) \quad (2)$$

where  $\Delta_{O,i}$  is the radial displacement at node  $i$  for overall OOC,  $\Delta_{I,i}$  is the radial displacement at node  $i$  for interframe OOC,  $a$  is the radius of the cylinder to the mid-plane of the shell plating,  $\theta$  is the angle at which the node is located in the Y-Z plane,  $\varphi$  is the phase angle for the OOC mode,  $L$  is the compartment length,  $L_B$  is the length between frames,  $x$  is the longitudinal coordinate of the node with origin at mid-length of the compartment, and  $x(\text{mod} L_B)$  is the remainder of  $x/L_B$ . The interframe OOC is applied only to the shell plating and the overall OOC is applied to the entire pressure hull. Figure 8 and Figure 9 show exaggerated views of the overall and interframe OOC, respectively for half of the compartment.

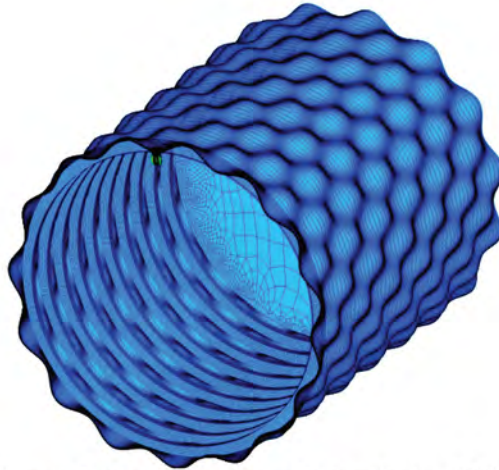


*Figure 8, Interframe out-of-circularity (500x)*

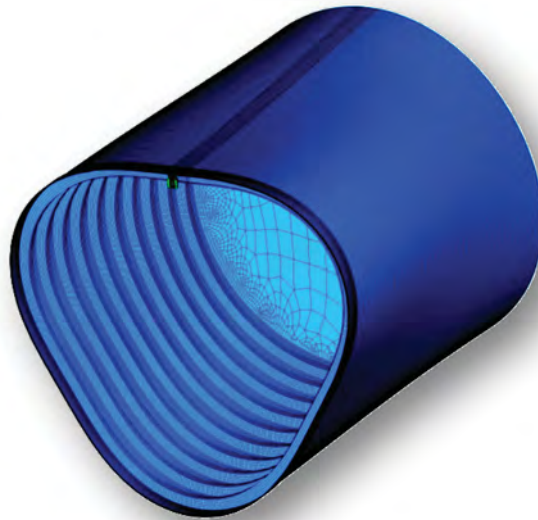


*Figure 9, Overall out-of-circularity (20x)*

## 2.4 Corrosion

Corrosion on the exterior of the pressure hull was modelled by deactivating a thin layer of solid elements on the outer surface of the shell plating using the ANSYS element birth and death feature. This feature "kills" elements by multiplying their stiffness by a severe reduction factor and removes any loads applied to those elements from the global load vector. The corrosion patch was square and its center was coincident with the center of the casting as shown in Figure 10, where mirror images were used to create a complete picture of the pressure hull. User-defined subroutines were written in the ANSYS parametric design language in order to create models with varying corrosion patch dimensions in much less time than would otherwise be required.



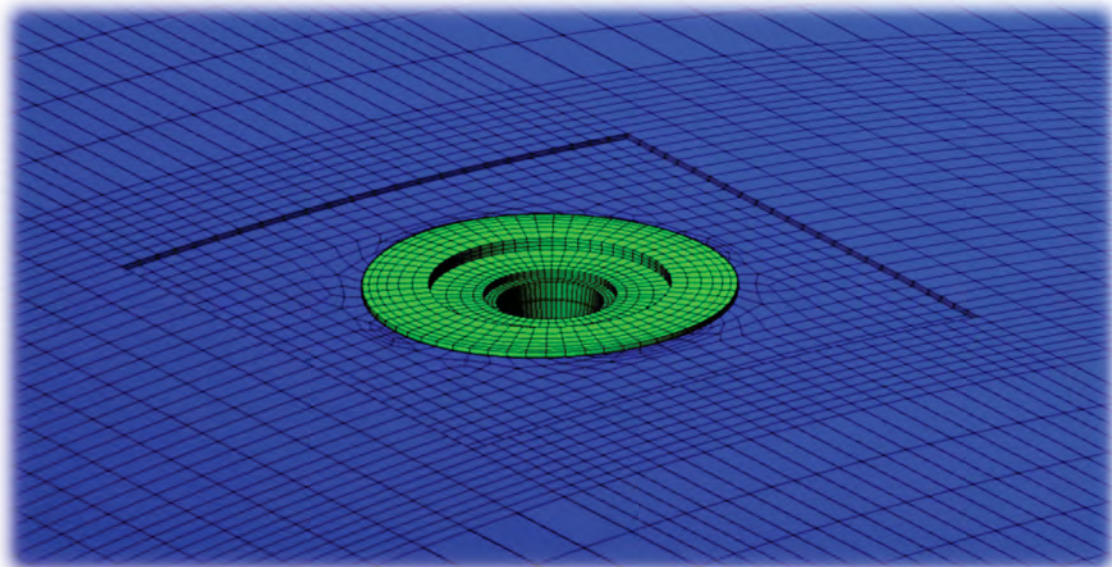


*Figure 10, Casting and corrosion patch*

## 2.5 Boundary Conditions and Loading

The finite element model was constrained using symmetry boundary conditions such that the model was symmetric about the X-Z and Y-Z planes as shown in Figure 11. Translations along the Y and Z axes were constrained for all bulkhead nodes. At the end of a compartment, boundary conditions are neither pinned nor clamped, but somewhere in between because of the restraint provided by pressure hull plating in the adjacent compartment. In order to provide a realistic amount of restraint to the shell plating at the ends of the compartment, 1.5 bays of plating with one stiffener were added on the outside of the bulkhead. At the end cross-section of this extra hull section, nodal rotations about the Y and Z axes were constrained and constraint equations were used to make displacements of all of the end cross-section nodes along the X-axis equal. These constraints on the end cross-section created a pseudo plane of symmetry that would allow axial displacements of the end cross-section when axial pressure loads are applied and provide a level of restraint consistent with that in a real pressure hull.

Pressure was applied to the exterior of the shell plating shell and solid elements, to the top surface of the casting, and to the interior of the casting that would be exposed to sea water when diving. A uniformly distributed axial load was applied to the end cross-section of the extra section that was added on the outside of the bulkhead to account for the axial pressure on the end closures. The magnitude of this pressure was  $Pr/2t$ , where  $P$  is the external hydrostatic pressure. The analysis considered material nonlinearity, large strains and large displacements so that pressure loads remain normal to the shell plating during deformation. The ANSYS automatic time stepping algorithm was used to bisect the load increment should the solution fail to converge.

during a substep. The minimum load increment allowed for automatic bisection was set to 1 Pa. Convergence failure of an analysis following this relatively low increment in applied load was indicative of buckling instability, at which point the analysis was concluded.

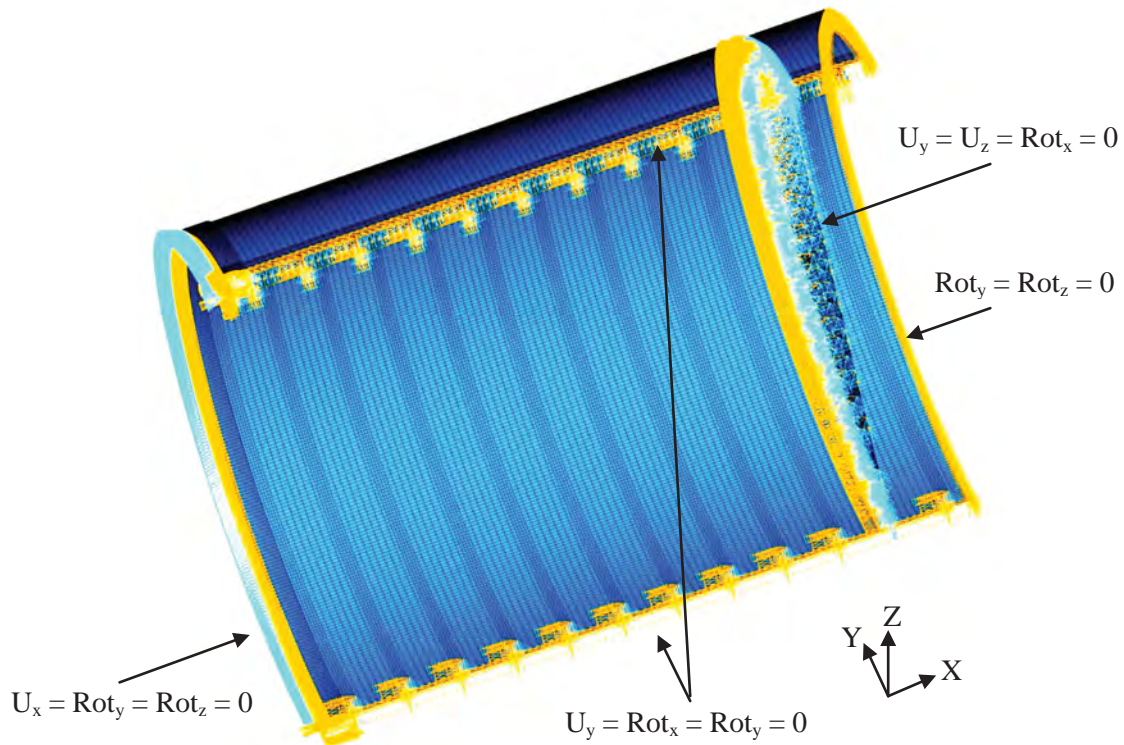


Figure 11, Displacement boundary conditions

## 2.6 Validation of the Modelling Method

In order to ensure that the solid to shell element transition in the finite element models did not adversely affect solution accuracy, collapse pressures of models meshed with solid and shell elements were compared with collapse pressures from ANSYS and SubSAS models meshed with shell elements only. The geometry of the models was the same as that shown in Figure 1 and all of the models included the same interframe and overall OOC imperfections, described in the previous section. For simplicity, none of the models used for validation included corrosion or a casting. A summary of collapse pressures, normalized with respect to the "ANSYS all shell" model is provided in Table 1. The variation in collapse pressure among the different models was small. The difference in collapse pressures predicted by models 1 and 2 is attributed to the different meshes and solution algorithms used by the two programs.

*Table 1, Collapse pressures predicted using different modelling methods*

Model type	Description	Normalized collapse pressure
1	SubSAS all shell	1.02
2	ANSYS all shell	1.00
3	ANSYS 1 bay of solids	1.00
4	ANSYS 3 bays of solids	0.99

## **2.7 Effect of Out-of-Circularity Phase Alignment**

Recognizing that the relative phases of the interframe and overall OOC modes may influence the possible resistance provided by the casting against interframe collapse, phases of the OOC modes were varied to ensure that a lower bound value is given for any increase in collapse pressure resulting from the presence of the casting. A model with a corrosion patch size of  $17t \times 17t$  with 15% thinning was used to investigate the influence of OOC phase alignment. Four ways of aligning the interframe and overall OOC are possible with the XZ symmetry plane:

1. Trough of overall and interframe OOC modes coincident with center of casting and corrosion patch;
2. Trough of overall OOC and crest of interframe OOC coincident with center of casting and corrosion patch;
3. Crest of overall and trough of interframe OOC coincident with center of casting and corrosion patch;
4. Crest of overall and interframe OOC coincident with center of casting and corrosion patch.

The failure load was taken as the pressure at which the radial displacement at the location of failure reached  $0.67t$ . Linear interpolation was used to obtain the pressure at  $0.67t$  displacement from adjacent data points. In cases where failure occurred at the casting, this relatively large displacement represents a serviceability limit state in that the movement of the casting would be accompanied by large deformations of the pipes connected to it. For cases 3 and 4, failure did not occur at the corrosion location, but by interframe buckling of the shell plating on the side of the pressure hull opposite the corrosion patch whether the casting was present or not. This can be attributed to the fact that the corrosion was located at a high spot in the pressure hull, lowering the neutral axis and reducing the effective out-of-circularity at that location. This effect may outweigh the reduction in collapse pressure caused by steel wastage in the corroded area [1]. For cases 1 and 2, failure occurred at the location of corrosion whether the casting was present or not. Figure 12 shows radial displacement at the center of the corrosion patch versus hydrostatic pressure for cases 1 and 2, where positive displacements are towards the center of the cylinder as illustrated in the deformed shape inset in the figure. Pressures in Figure 12 are normalized with respect to the collapse pressure for the undamaged type 3 model. The presence of the casting resulted in similar increases in collapse pressure for cases 1 and 2 of approximately 11% and 9%, respectively. Based on these results, OOC phase alignment case 1 was chosen for all subsequent analyses.

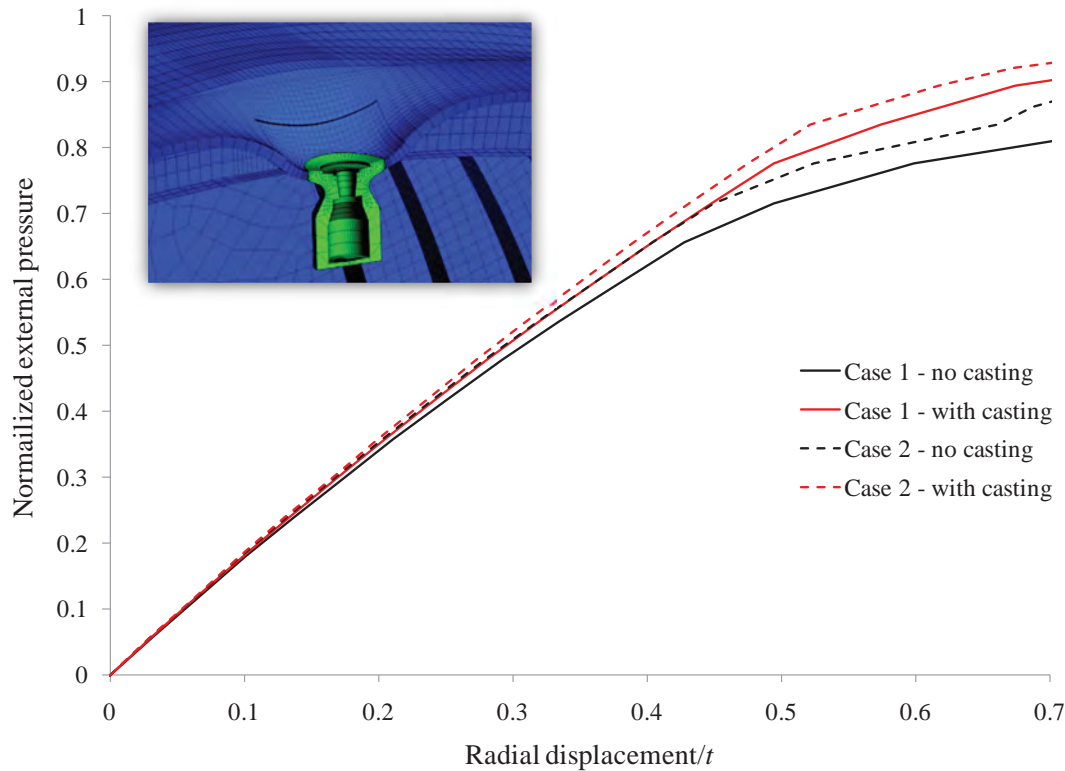


Figure 12, Radial displacement at the center of the corrosion patch.

## 2.8 Simplifying the casting geometry

Modelling a penetration and casting in a pressure hull using solid elements is a time-consuming process due to the time required to model the casting and to create solid to shell element connections. The time required for solution also increases significantly due to the greater number of elements used compared to a model meshed entirely with shell elements. An alternative to modelling the casting with solid elements is to use shell elements with a thickness equal to the average thickness of the casting wall. Corrosion can then be modelled by reducing the thickness of selected elements in the damaged area and offsetting the nodes in those elements so that the inner surface of the shell plating under the corrosion patch remains flush with the rest of the inner surface of the pressure hull. Figure 13 shows the corroded portion of the pressure hull with the simplified casting model where the left and right sides of the figure, respectively show the shell elements with and without their thickness displayed.

A finite element model consisting of all shell elements and using a simplified casting geometry was created considering a  $17t \times 17t$  corrosion patch with 15% thinning of the pressure hull material. Results of that analysis were compared with results from analysis of a model using both solid and shell elements (model type 3 in Table 1) as shown inset in Figure 12 and described in Section 2.1. Both models failed by interframe buckling at the location of the casting and corrosion patch. Figure 14 shows a comparison of load versus radial displacement of the valve for the two models. The lower fidelity, all shell model was able to sustain a pressure 7% higher than the type 3 model, however the softer response of the simplified model could indicate a serviceability limit



state at a lower pressure than the more detailed solid/shell model. This could result in overly conservative limits on allowable diving depth based on serviceability requirements. For example, if displacements greater than  $0.67t$  result in valve malfunction, the allowable normalized pressure would be 0.8 based on an analysis using the simplified model versus 0.89 for the solid/shell model. Considering the significant differences in behaviour caused by simplification of the casting geometry, the higher fidelity, type 3 and type 4 models are used for the parametric study.

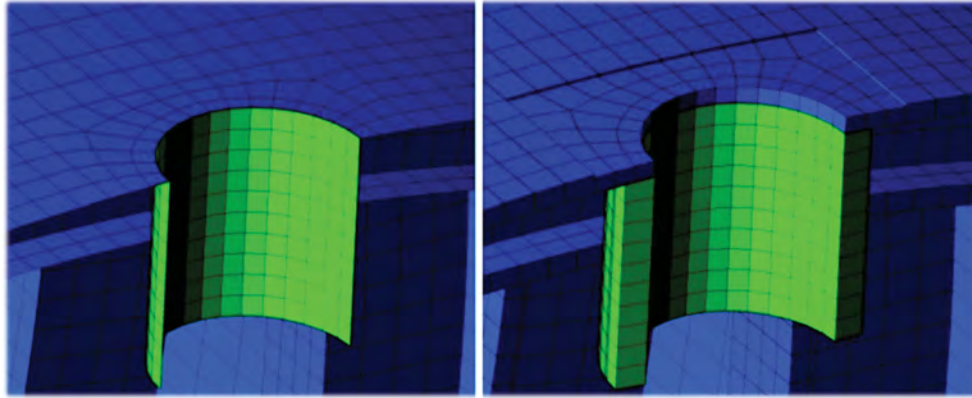


Figure 13, Simplified casting geometry

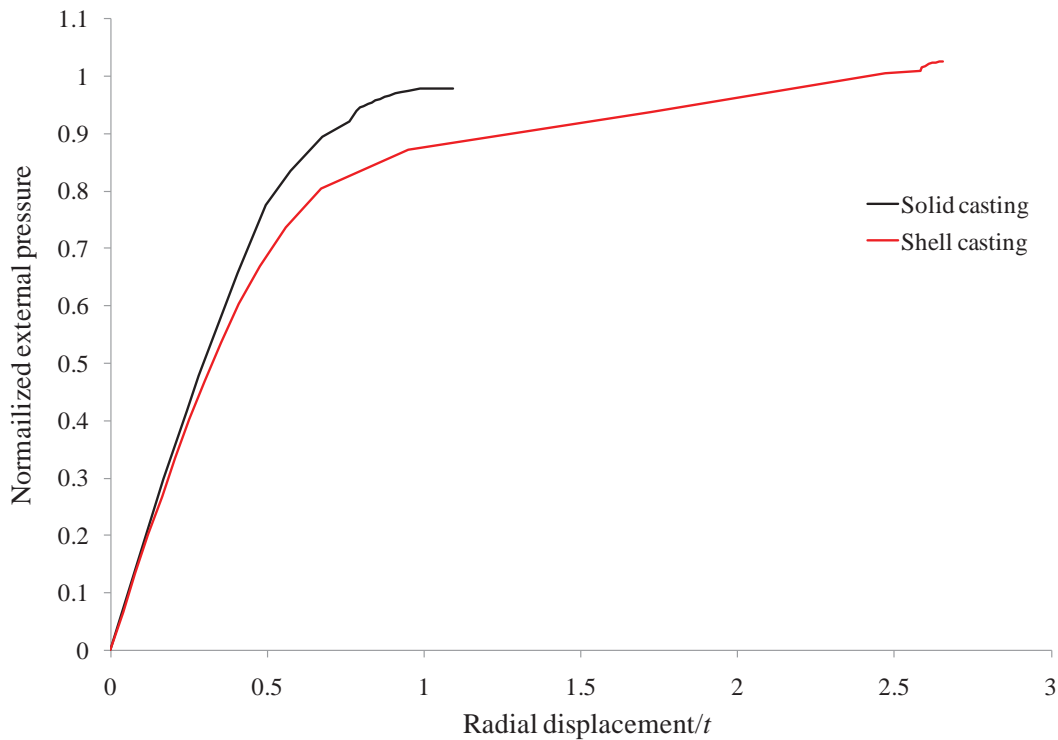
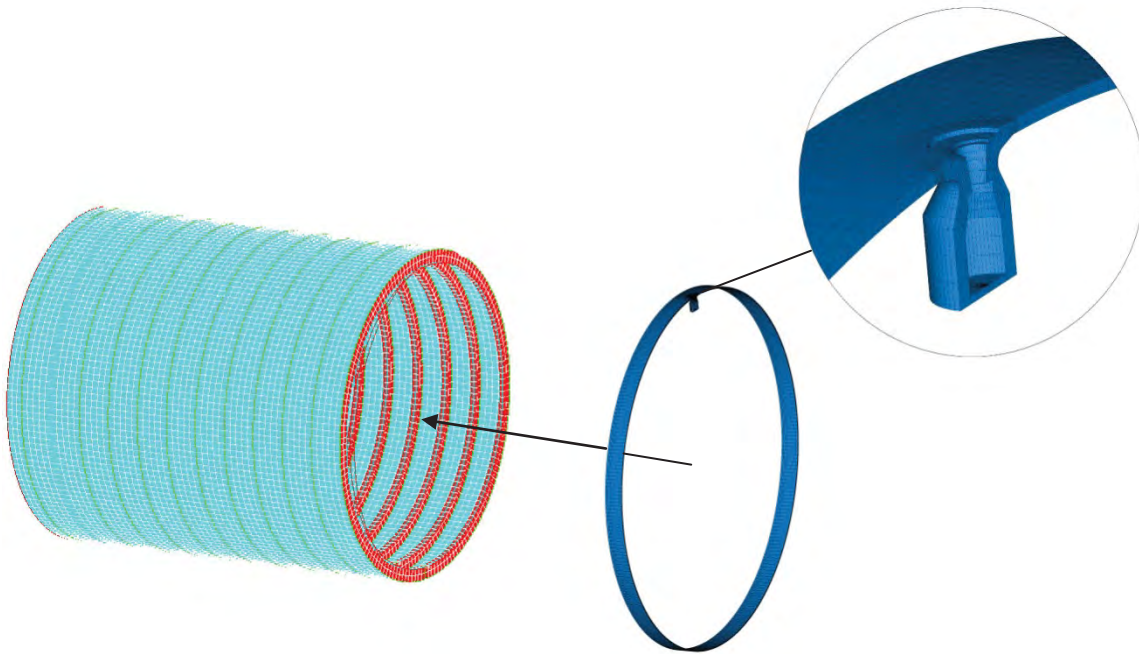


Figure 14, Radial displacement of casting

## 2.9 SubSAS Modelling

The Submarine Structural Analysis Software (SubSAS) program [6], developed by DRDC and the UK MoD was evaluated for its ability to analyze a pressure hull with a penetration and casting included. The same casting, pressure hull geometry and material properties described in the previous sections were considered. The SubSAS modeller, and the Trident and ANSYS finite element programs were used to try to combine a solid element mesh from ANSYS with a shell element mesh created using SubSAS for analysis using the VAST finite element solver. The ANSYS program was used to model the relatively complicated geometry of the casting and surrounding corrosion patch. SubSAS was not suited to this task because it is not a general purpose finite element modelling program. The solid element mesh from ANSYS was similar to that described in the previous sections where the casting, corrosion patch and the rest of the surrounding shell plating up to the nearest ring frame were meshed with 8-node hexahedrons. For use in the SubSAS mesh, the solid model consisted of a complete ring of shell plating, instead of using symmetry to model only half of the circumference. The rest of the pressure hull was modelled in SubSAS and meshed with shell elements only. Figure 15 shows how the two finite element meshes were joined.



*Figure 15, Joining of ANSYS and SubSAS finite element models*

Joining the two finite element models for a collapse analysis was accomplished as follows:

1. Following creation of the ANSYS, solid element part of the finite element (FE) model, the ANSYS parametric design language (APDL) command, `CDWRITE,db,<filename>,inp` was used to write the ANSYS FE model to a file with the .inp extension.

2. The .inp file was placed in a new working directory created for a Trident model and imported into Trident.
3. After import into Trident, the FE model was exported to a .gom file and that file was moved to a working directory created for the SubSAS analysis.
4. The shell element portion of the FE model was created in SubSAS.
5. The path to the external mesh (.gom file), originally created in ANSYS, was entered in the SubSAS analysis type wizard and preprocessing of the model in SubSAS was performed to import the external mesh. The combined solid/shell model was saved to a .gom file.
6. The .gom file created by SubSAS was imported into Trident.

The SubSAS program successfully combined an externally generated hexahedral mesh model with the SubSAS shell element mesh, however some difficulties were encountered when applying boundary conditions and when connecting the two FE meshes using multi-point constraints (MPCs). The shortcomings of SubSAS in implementing a pressure hull analysis with a portion of the model consisting of an externally generated hexahedral FE mesh are outlined in the following.

1. Although pressure loads on the shell elements of the SubSAS model were carried over from SubSAS to Trident, they were not applied to the externally generated, solid element part of the model. It was difficult to apply pressure loads to the surface of the solid elements on the exterior face of the shell plating in Trident because those elements could not easily be selected to apply the loads. As a work-around, thin shell elements were overlaid on the external faces of the solid elements in the ANSYS model before it was exported so that the pressure load could be applied to those shell elements once the combined model was imported from SubSAS into Trident. Unfortunately, SubSAS did not recognize the shell elements when the ANSYS model was imported.
2. The SubSAS method of generating out-of-circularity imperfections saved a significant amount of time compared to generating the OOC in a general purpose FE program such as ANSYS. However, when an external mesh was imported, SubSAS did not apply the OOC to the externally meshed part of the model. This means that the OOC must be applied to the externally meshed model before it is imported into SubSAS, which can be arduous considering that the OOC in both the SubSAS model and the external model must be aligned so that they fit together properly when combined in SubSAS.
3. When the combined SubSAS model was imported into Trident for analysis, MPCs were generated to connect the solid and shell element meshes together. Although the Trident graphical user interface indicated that the MPCs existed at the interface between the two meshes, when the analysis was run, the MPCs did not function and rigid body motion resulted in failure of the solver.
4. Axial loads accounting for pressure on the end closures of the hull were applied to both ends of the shell part of the model, but not to the part meshed with solid elements. Also, the symmetry boundary condition specified at the compartment mid-length in SubSAS was not transferred to the solid element mesh.

Due to these difficulties in incorporating an externally meshed object in a SubSAS/Trident FE analysis, the ANSYS finite element package was used for all subsequent modelling. The ANSYS parametric design language was used to create user-defined subroutines for model creation, meshing, generation of the OOC, application of boundary conditions and solution. Although the ANSYS FE program is a powerful tool, it requires a considerable amount of experience in finite element modelling and familiarity with the program to create and analyze pressure hull models. For analysis of stiffened cylinders not requiring detailed hexahedral meshes in parts of the model, the streamlined SubSAS modelling approach is still preferable for producing and analyzing pressure hull models in much less time than would be required using a general purpose finite element program. Although there are some deficiencies in the SubSAS capability to import externally generated hexahedral meshes and to use them in a structural analysis, the functionality does exist and will be improved upon in the future.

### 3 Parametric Study

A parametric study was carried out to determine how the presence of a casting within a corrosion patch affects a serviceability limit state considering various corrosion patch geometries. Failure was assumed to occur when the radial deflection at the center of the corrosion patch reached  $0.7t$ . The dimensions of the corrosion patch areas considered were  $17t \times 17t$ ,  $25t \times 25t$  and  $33t \times 33t$ , where one dimension is the length of the patch in the fore-aft direction and the other is the length of the patch measured around the outside circumference of the shell plating. The depth of the corrosion patch was also varied, ranging from 5% to 20% of the shell plating thickness in increments of 5%. A summary of failure pressures for each corrosion patch geometry considered is given in Table 2, where pressures have been normalized with respect to the serviceability limit state pressure for the same pressure hull geometry with the casting, but with no corrosion damage. Table 3 shows the percentage increase in the serviceability limit state due to the presence of the casting for each case and provides the percentage change in the serviceability limit state due to corrosion for the pressure hull with the casting. Table 4 shows the reduction in failure load due to corrosion with the casting included in all analyses. From comparison of these results with those in Table 2, where the failure loads with and without the casting are given, it is evident that the casting has negligible influence on failure load when there is no corrosion damage.

*Table 2, Normalized collapse pressures*

No.	Corrosion Patch Size	Model ID	% Thinning*			
			5	10	15	20
1	$17t \times 17t$	1	0.94 / 0.98	0.87 / 0.94	0.81 / 0.90	0.76 / 0.86
2	$25t \times 25t$	1	0.94 / 0.97	0.87 / 0.92	0.78 / 0.89	0.70 / 0.83
3	$33t \times 33t$	2	0.94 / 0.99	0.89 / 0.94	0.80 / 0.88	0.72 / 0.85

\* no casting / with casting

*Table 3, Increase in failure load due to presence of casting (%)*

No.	% Thinning			
	5	10	15	20
1	3.41	8.05	11.53	12.96
2	3.28	5.06	14.16	18.35
3	5.27	5.41	10.18	18.71

*Table 4, Decrease in failure load due to corrosion including casting (%)*

No.	% Thinning			
	5	10	15	20
1	2.48	6.28	9.73	14.47
2	3.20	8.35	11.50	16.71
3	1.25	6.08	11.94	14.94

Results indicate that the presence of the casting increases collapse pressure to a greater degree as the depth of the corrosion patch increases. There does not appear to be any correlation between the size of the corroded area and the influence of the casting on collapse pressure. Figure 16 shows the response of the pressure hull at the center of corrosion patch No. 2 with 15% thinning with and without a casting. It is evident from the figure that the casting stiffens the shell plating slightly until the displacement reaches approximately  $0.4t$ . Beyond that point, the influence of the casting becomes more pronounced, increasing the load-carrying capacity by 14% at a radial displacement of  $0.7t$  and by approximately 11% from a displacement of  $t$  to  $1.8t$ . Following interframe buckling, indicated by the long plateau in the curves, in both cases there was a further increase in load-carrying capacity as a yielding progressed through the thickness of the plating near the casting and further applied load is transferred to the surrounding structure through membrane stresses in the shell plating at the failure location. Although the difference between the ultimate loads was only around 2% at the ultimate load, the excessive displacements would exceed the serviceability limit state. Furthermore, at such high strains, necking and fracture may occur at which point the material model used in the analysis would no longer be valid. Load versus displacement curves for the other cases considered in Table 3 are included in Annex A.

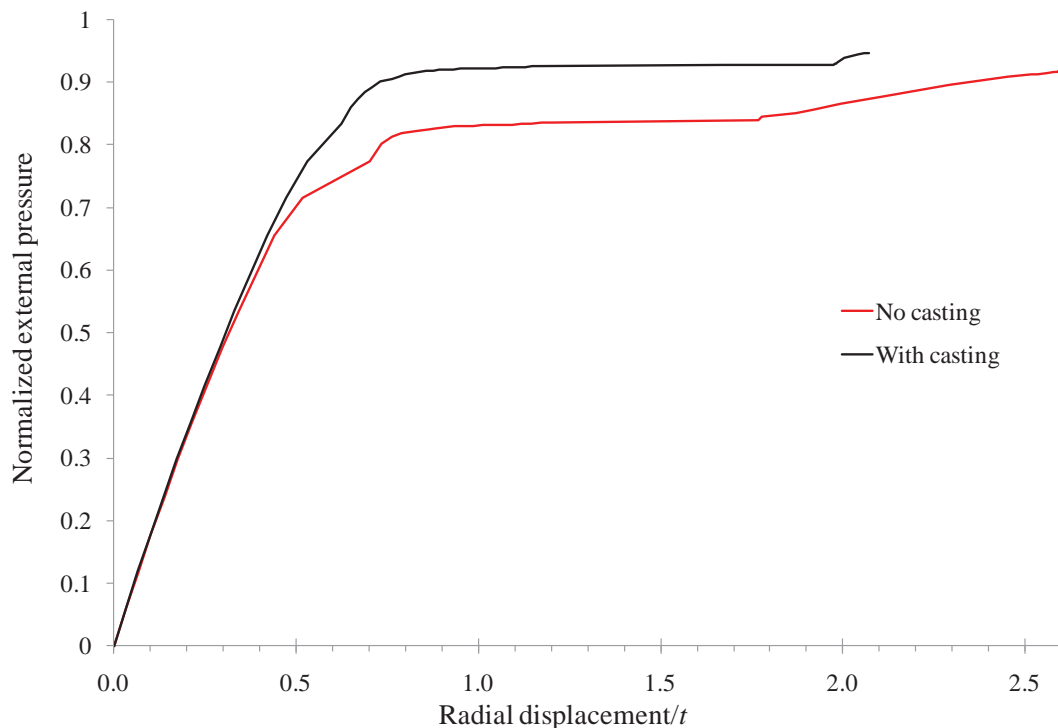


Figure 16, Radial displacement at center of corrosion patch No. 2 with 15% thinning

## 4 Conclusions

---

Various methods of modelling a penetration and casting within a submarine pressure hull were evaluated using finite element analysis. A comparison of model results showed that a pressure hull with a casting can be effectively modelled using a combination of solid and shell elements joined by beam elements. A parametric study was carried out using this model type to study the effect of including a casting within a corrosion patch on interframe buckling behaviour. Several corrosion patch sizes and percentages of shell plating thinning due to corrosion were considered.

A comparison of different casting modelling methods showed that using shell elements to simplify the casting model results in an underestimate of the shell plating stiffness in the corroded area, giving conservative values for failure loads considering a serviceability limit state. The higher fidelity model wherein the casting and surrounding area were meshed using solid elements was then used in the parametric study. It was found that the presence of the casting increased the failure load above that of the corroded hull with no casting by 3% to 19% and that the benefit provided by the casting increased as the percentage thinning of the shell plating due to corrosion increased. This means that where corrosion-related structural failure occurs near a casting, structural performance is not adversely affected by the presence of the casting. In fact, the influence of a casting and penetration on pressure hull behaviour near corrosion is significant and should be considered in a numerical analysis if practicable.

An attempt was made to carry out the pressure hull analysis using SubSAS, where SubSAS was used to create a finite element model for the majority of the pressure hull using shell elements, and the ANSYS finite element program was used to create a solid element mesh of the casting and surrounding area. The ANSYS mesh was successfully imported into SubSAS, however some difficulties were encountered with application of the OOC, boundary conditions and in joining the two meshes using multi-point constraints. Although it is possible to automate the application of boundary conditions and creation of MPCs in a combined solid/shell model in SubSAS, it may be overly optimistic to assume that this can be done in such a way that a wide range of different solid element meshes can be imported into SubSAS and analyzed with little user intervention.

## References

---

- [1] Smith, M.J. and MacKay, J.R. (2005). Overall elasto-plastic collapse of ring stiffened cylinders with corrosion damage. *Transactions of the Royal Institution of Naval Architects Part 1A - International Journal of Maritime Engineering*.
- [2] Jiang, L., MacKay, J.R., Wallace, J., Smith, M.J., Norwood, M., Bosman, T. (2008). Finite element modelling of collapse experiments of ring stiffened cylinders with simulated corrosion damage. In *Warship 2008: Naval Submarines 9*. Glasgow: Royal Institution of Naval Architects.
- [3] MacKay, J.R. (2007). Experimental investigation of the strength of damaged pressure hulls - Phase 1. (DRDC Atlantic TM 2006-304). Defence Research and Development Canada - Atlantic.
- [4] Defence Procurement Agency (2001). SSP 74 Design of Submarine Structures. Sea Systems Publication No. 74. Defence Procurement Agency, Sea Technology Group, United Kingdom.
- [5] Bayley, C. (2007). Stress-Strain Characterization of NQ1 Pressure Hull Material. (DRDC Atlantic TN 2007-328). Defence Research and Development Canada - Atlantic.
- [6] Pegg, N.G. and Heath, D.C. (2001). Submarine Structural Analysis Suite, SubSAS Phase 1. (DREA TM 2001-025). Defence Research Establishment Atlantic.



## Annex A Load Versus Displacement Curves

### A.1 5% Thinning of Shell Plating

All plots that follow have pressures normalized with respect to the collapse pressure of the same model type with no corrosion or casting, as given in Table 1.

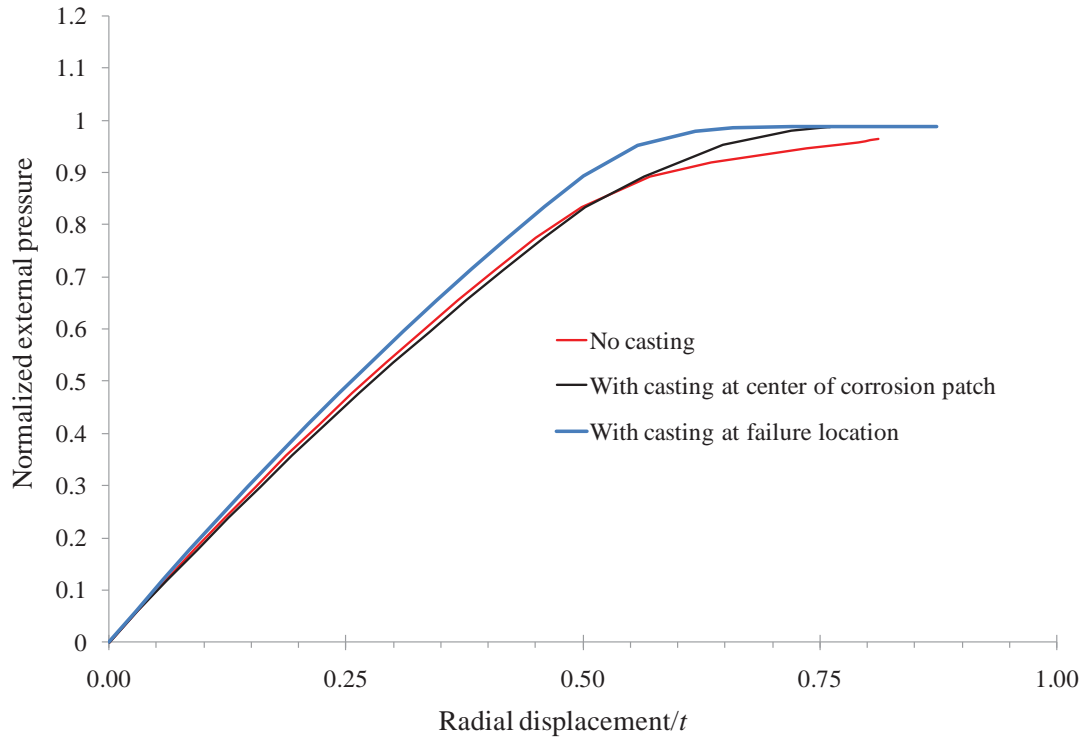


*Figure A-1, Radial displacement for corrosion patch No. 1*

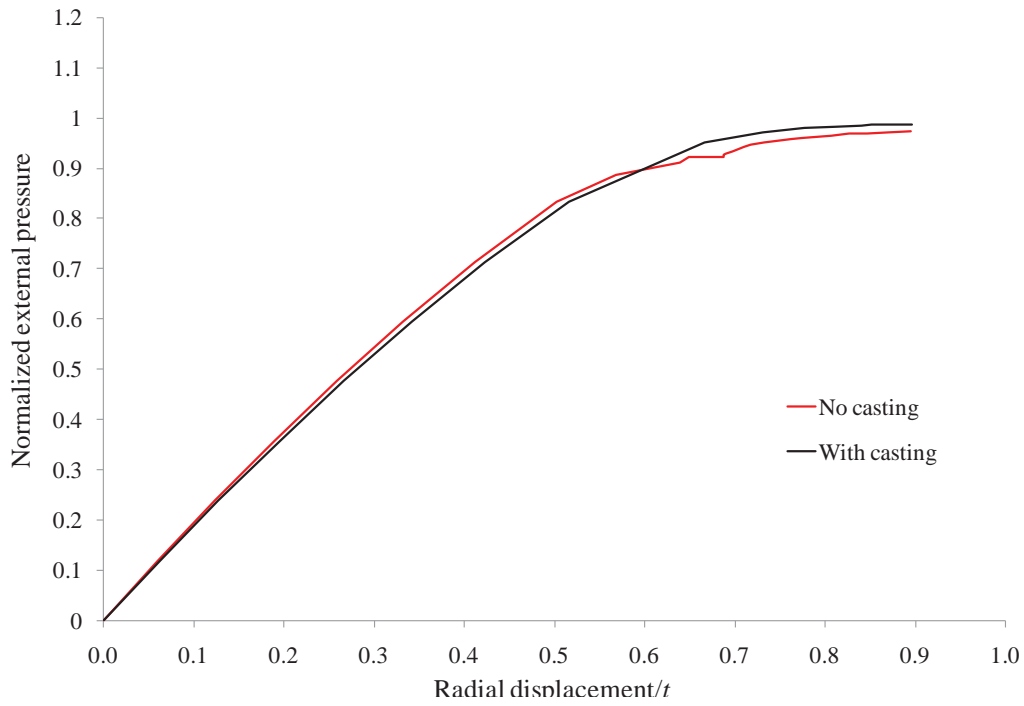


Figure A-2, Radial displacement at center of corrosion patch for corrosion patch No. 2

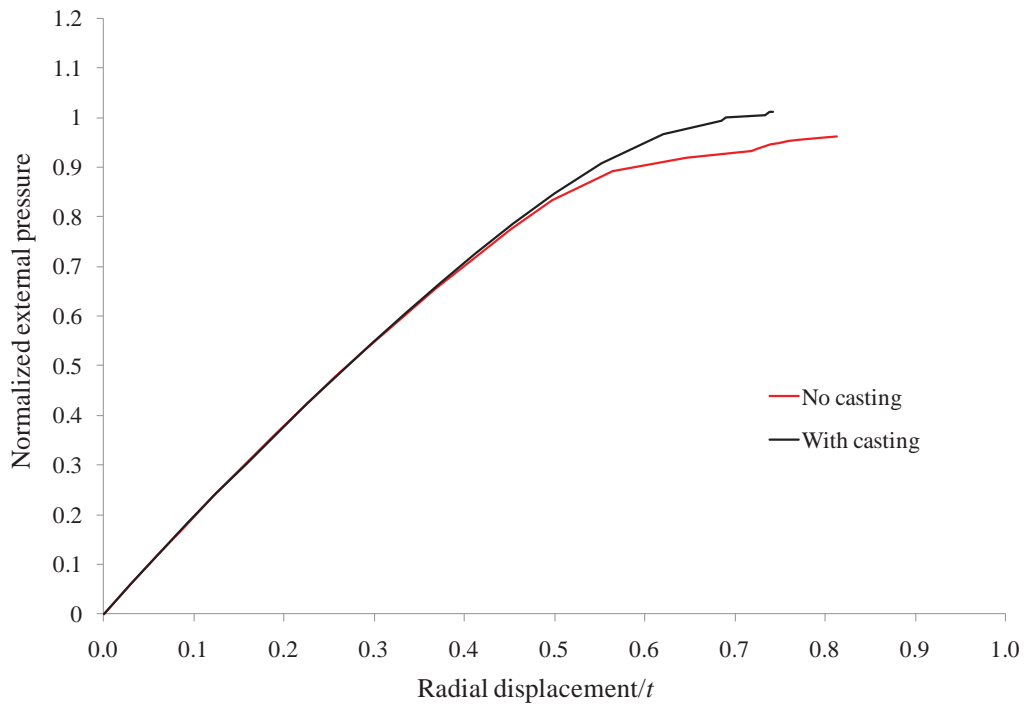


Figure A-3, Radial displacement at center of corrosion patch for corrosion patch No. 3

## A.2 10% Thinning of Shell Plating

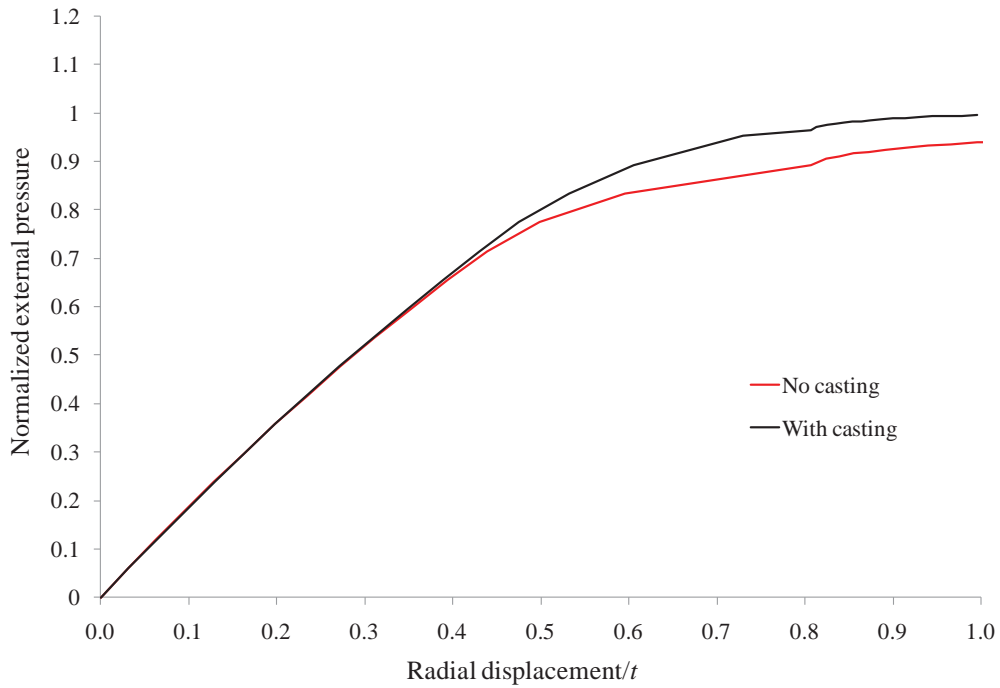


Figure A-4, Radial displacement at center of corrosion patch for corrosion patch No. 1

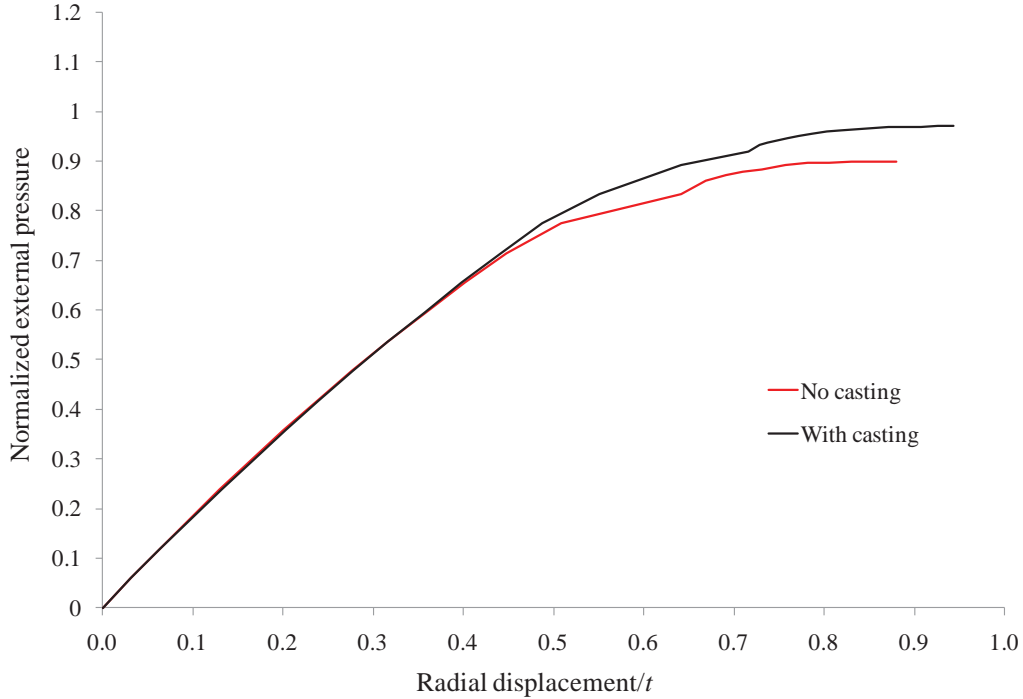


Figure A-5, Radial displacement at center of corrosion patch for corrosion patch No. 2

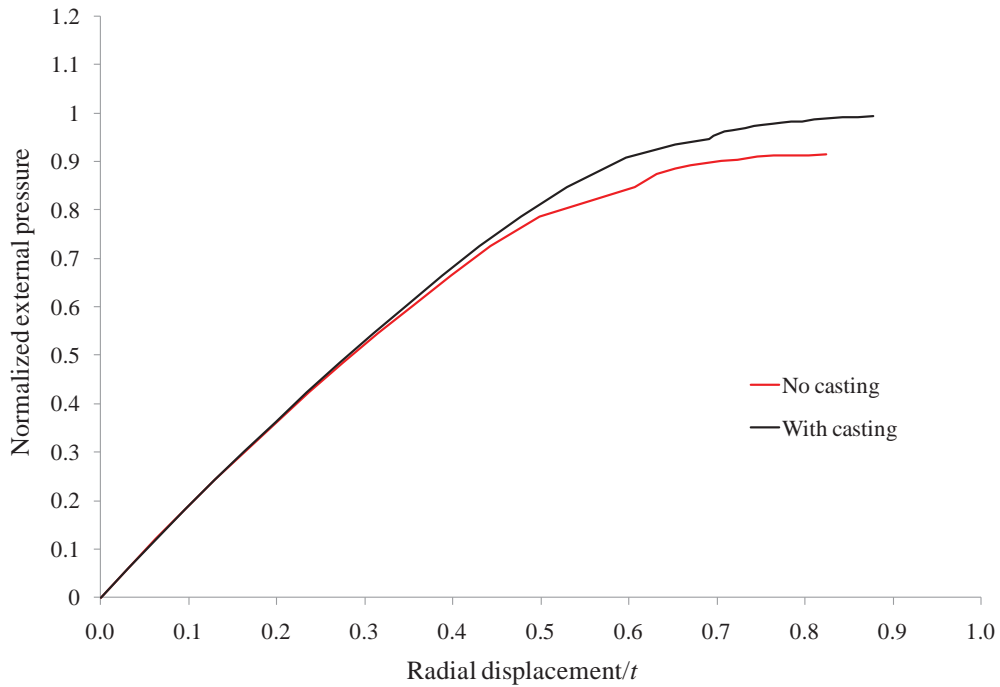


Figure A-6, Radial displacement at center of corrosion patch for corrosion patch No. 3

### A.3 15% Thinning of Shell Plating

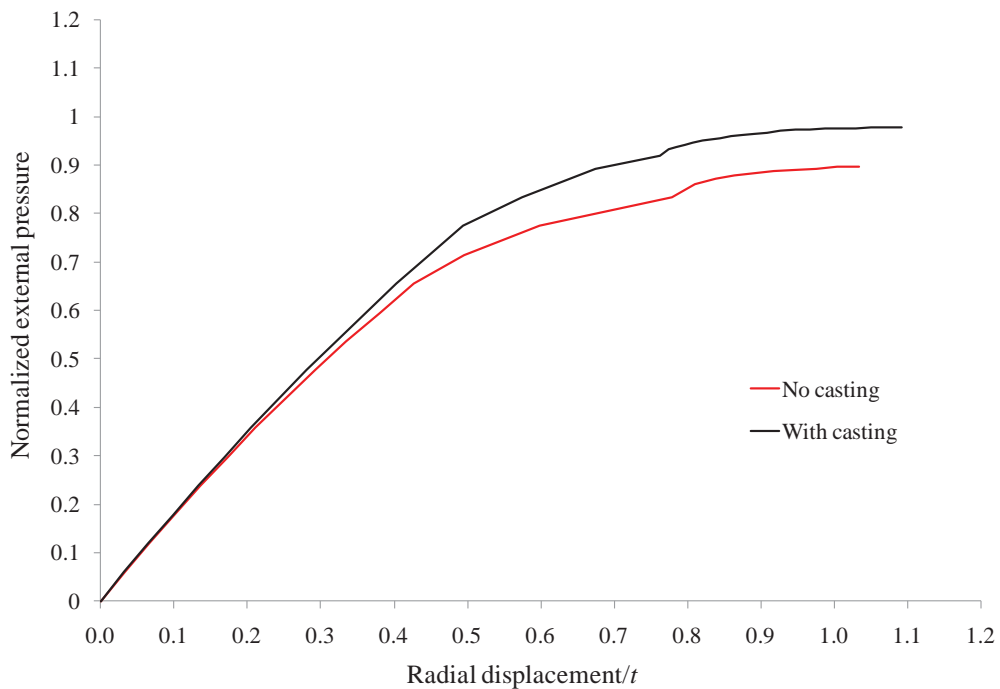


Figure A-7, Radial displacement at center of corrosion patch for corrosion patch No. 1

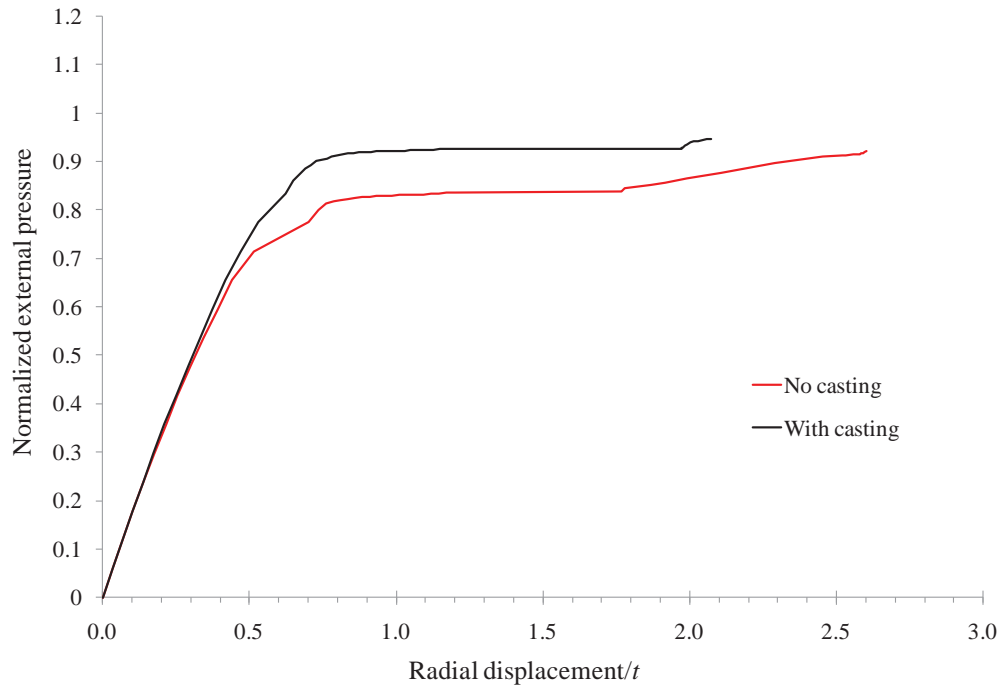


Figure A-8, Radial displacement at center of corrosion patch for corrosion patch No. 2

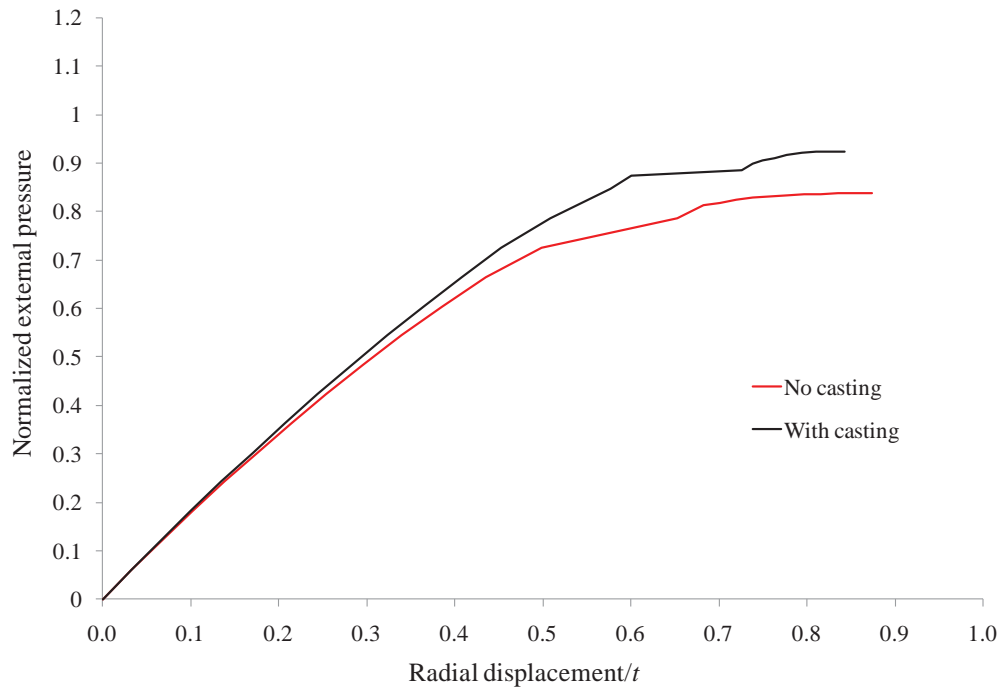


Figure A- 9, Radial displacement at center of corrosion patch for corrosion patch No. 3

#### A.4 20% Thinning of Shell Plating

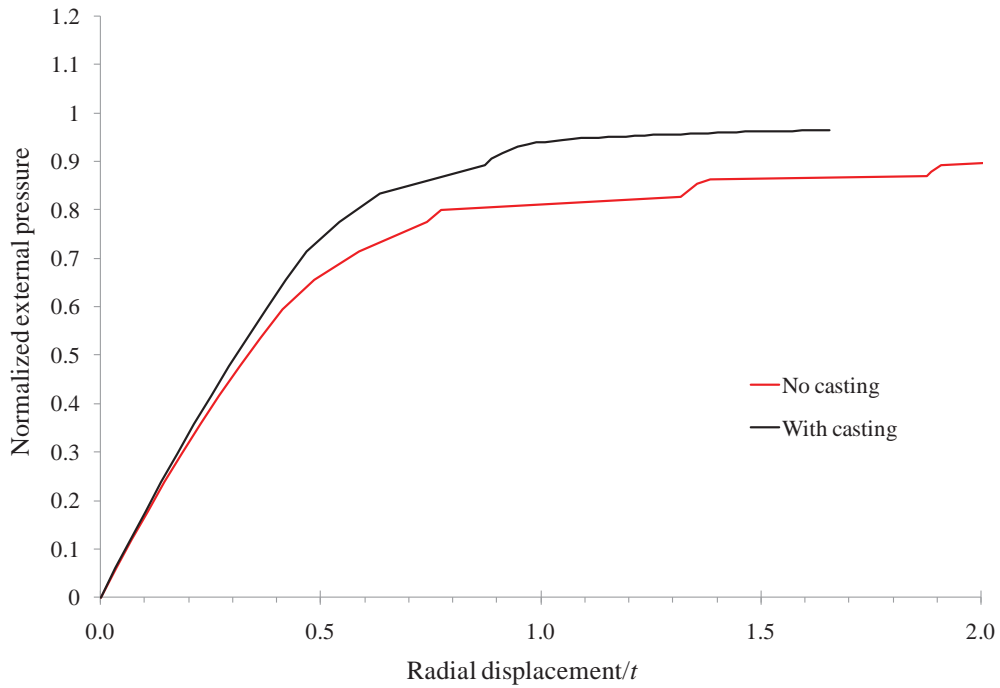


Figure A-10, Radial displacement at center of corrosion patch for corrosion patch No. 1

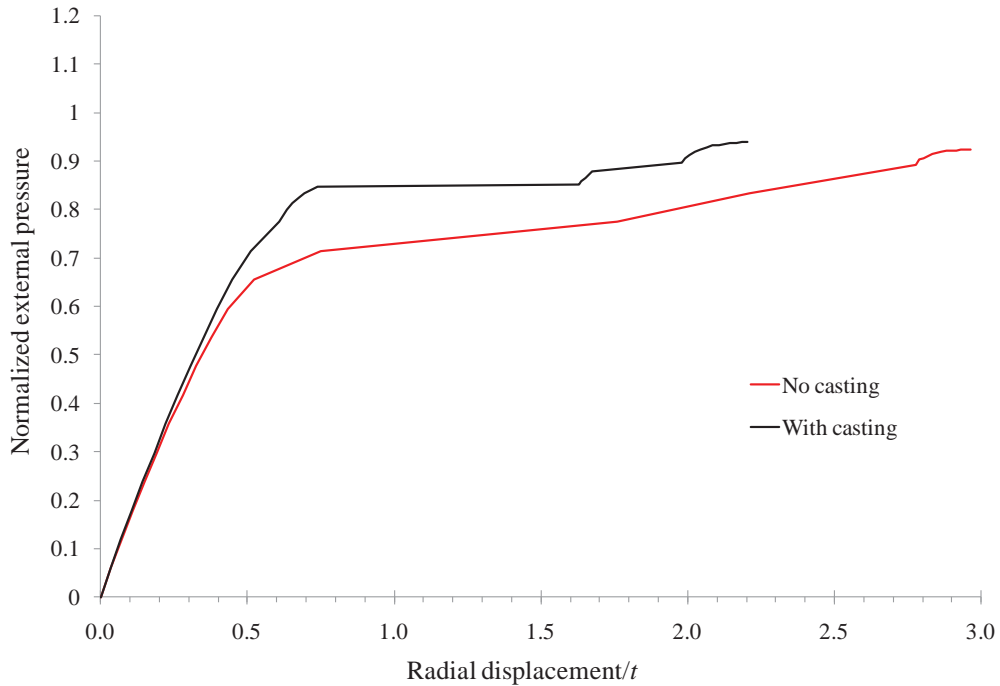


Figure A-11, Radial displacement at center of corrosion patch for corrosion patch No. 2

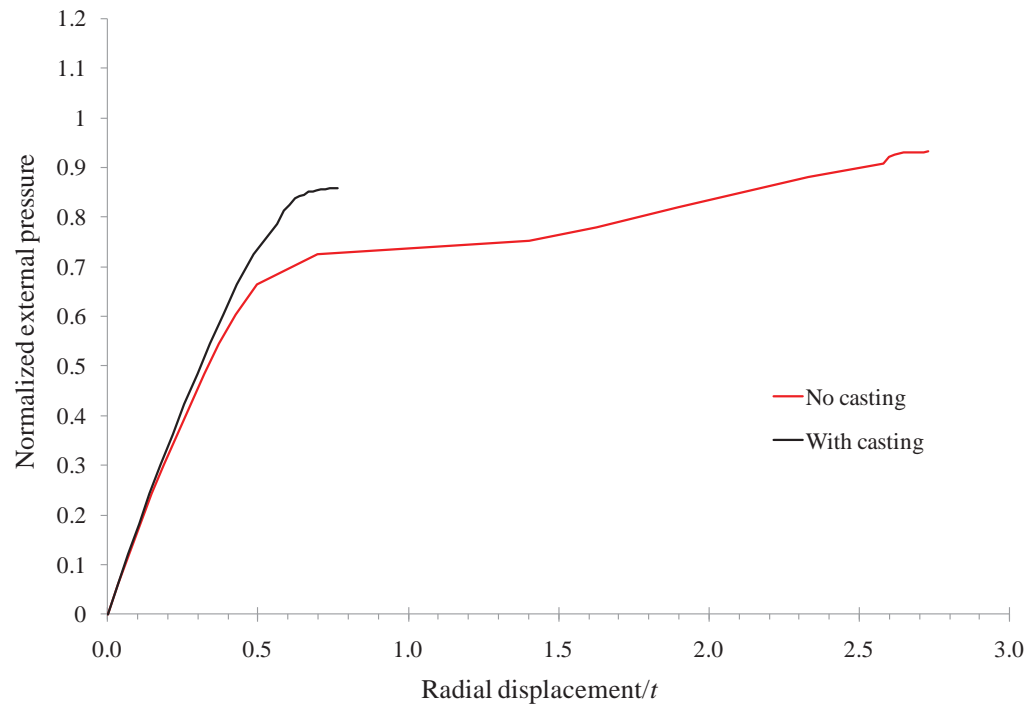


Figure A-12, Radial displacement at center of corrosion patch for corrosion patch No. 3

This page intentionally left blank.



## List of symbols/abbreviations/acronyms/initialisms

---

### Symbols

$A_I$	Amplitude of interframe out-of-circularity
$A_O$	Amplitude of overall out-of-circularity
$a$	Radius of cylinder to mid-plane of shell plating
$L$	Compartment length
$L_B$	Bay length
mod	modulo
$n$	Out-of-circularity mode number
$r$	Radius of cylinder to outside of shell plating
$rot_x, rot_y, rot_z$	Rotations about X, Y and Z axes, respectively
sin	sine
$t$	Shell plating thickness
$u_x, u_y, u_z$	Displacements in X, Y and Z directions, respectively
$x, y, z$	Cartesian coordinate axes
$\theta$	Angle to node location in Y-Z plane
$\varphi$	Phase angle for OOC

### Abbreviations, acronyms and initialisms

DND	Department of National Defence
DRDC	Defence Research & Development Canada
DRDIM	Director Research and Development Knowledge and Information Management
OOC	Out-of-circularity
R&D	Research & Development
SSP	Sea Systems Publication
SubSAS	Submarine Structural Analysis Software

This page intentionally left blank.

## Distribution list

---

Document No.: DRDC Atlantic TM 2010-246

### **LIST PART 1 – Internal Distribution by Centre:**

- 4 Author (2 paper copies, 2 CDs)
- 3 DRDC Atlantic Library (1 paper copies, 2 CDs)
- 1 Scientific Authority, Submarine Scientific Support SLA (Mr. John Porter)
- 1 Project Manager, Submarine Scientific Support SLA (LCdr Wade Temple)
  
- 9 *TOTAL LIST PART I*

### **LIST PART II: External Distribution within Canada by DRDKIM**

- 1 NDHQ/DRDKIM 3
- 2 NDHQ/DMEPM(SM) 4
- 2 NDHQ/DMEPM(SM) 4-2
- 1 Library and Archives Canada (Attn: Military Archivist, Government Records Branch)
  
- 6 *TOTAL LIST PART II*

**15 TOTAL COPIES (3 paper copies, 12 CDs)**

This page intentionally left blank.

DOCUMENT CONTROL DATA		
(Security classification of title, body of abstract and indexing annotation must be entered when the overall document is classified)		
1. ORIGINATOR (The name and address of the organization preparing the document. Organizations for whom the document was prepared, e.g. Centre sponsoring a contractor's report, or tasking agency, are entered in section 8.)  Defence R&D Canada – Atlantic 9 Grove Street P.O. Box 1012 Dartmouth, Nova Scotia B2Y 3Z7	2. SECURITY CLASSIFICATION (Overall security classification of the document including special warning terms if applicable.)  UNCLASSIFIED	
3. TITLE (The complete document title as indicated on the title page. Its classification should be indicated by the appropriate abbreviation (S, C or U) in parentheses after the title.)  Submarine Pressure Hull Collapse Considering Corrosion and Penetrations		
4. AUTHORS (last name, followed by initials – ranks, titles, etc. not to be used)  Gannon, L		
5. DATE OF PUBLICATION (Month and year of publication of document.)  November 2010	6a. NO. OF PAGES (Total containing information, including Annexes, Appendices, etc.)  44	6b. NO. OF REFS (Total cited in document.)  6
7. DESCRIPTIVE NOTES (The category of the document, e.g. technical report, technical note or memorandum. If appropriate, enter the type of report, e.g. interim, progress, summary, annual or final. Give the inclusive dates when a specific reporting period is covered.)  Technical Memorandum		
8. SPONSORING ACTIVITY (The name of the department project office or laboratory sponsoring the research and development – include address.)  Defence R&D Canada – Atlantic 9 Grove Street P.O. Box 1012 Dartmouth, Nova Scotia B2Y 3Z7		
9a. PROJECT OR GRANT NO. (If appropriate, the applicable research and development project or grant number under which the document was written. Please specify whether project or grant.)  11GX03	9b. CONTRACT NO. (If appropriate, the applicable number under which the document was written.)	
10a. ORIGINATOR'S DOCUMENT NUMBER (The official document number by which the document is identified by the originating activity. This number must be unique to this document.)  DRDC Atlantic TM 2010-246	10b. OTHER DOCUMENT NO(s). (Any other numbers which may be assigned this document either by the originator or by the sponsor.)	
11. DOCUMENT AVAILABILITY (Any limitations on further dissemination of the document, other than those imposed by security classification.)  Unlimited		
12. DOCUMENT ANNOUNCEMENT (Any limitation to the bibliographic announcement of this document. This will normally correspond to the Document Availability (11). However, where further distribution (beyond the audience specified in (11) is possible, a wider announcement audience may be selected.)  Unlimited		

13. **ABSTRACT** (A brief and factual summary of the document. It may also appear elsewhere in the body of the document itself. It is highly desirable that the abstract of classified documents be unclassified. Each paragraph of the abstract shall begin with an indication of the security classification of the information in the paragraph (unless the document itself is unclassified) represented as (S), (C), (R), or (U). It is not necessary to include here abstracts in both official languages unless the text is bilingual.)

The influence of corrosion around a casting in a submarine pressure hull is investigated using nonlinear finite element modelling techniques. The area encompassed by the corrosion patch and the percentage thinning of the pressure hull due to corrosion are varied. For each variation in corrosion patch dimensions, collapse pressures are calculated with and without a ballast pump valve body casting located at the center of the corrosion patch. The extent to which the presence of the casting within a corrosion patch influences collapse pressure is examined and different methods of modelling the casting within the pressure hull are evaluated. The loss of strength caused by corrosion is largely counteracted by the presence of a casting in the corroded region. The casting stiffens the response of the shell plating in that area, causing an increase in collapse pressure. The benefit provided by the casting increased as the percentage thinning of the shell plating increased, increasing the failure load of the corroded hull by as much as 19% for 20% thinning of the shell plating.

14. **KEYWORDS, DESCRIPTORS or IDENTIFIERS** (Technically meaningful terms or short phrases that characterize a document and could be helpful in cataloguing the document. They should be selected so that no security classification is required. Identifiers, such as equipment model designation, trade name, military project code name, geographic location may also be included. If possible keywords should be selected from a published thesaurus, e.g. Thesaurus of Engineering and Scientific Terms (TEST) and that thesaurus identified. If it is not possible to select indexing terms which are Unclassified, the classification of each should be indicated as with the title.)

submarine structures; corrosion; castings, nonlinear finite element analysis; pressure vessel

This page intentionally left blank.

## **Defence R&D Canada**

Canada's leader in defence  
and National Security  
Science and Technology

## **R & D pour la défense Canada**

Chef de file au Canada en matière  
de science et de technologie pour  
la défense et la sécurité nationale



[www.drdc-rddc.gc.ca](http://www.drdc-rddc.gc.ca)